Engineering and Technology Journal
Journal homepage: https://etj.uotechnology.edu.iq

Desulfurization of Real Diesel Fuel onto Mesoporous Silica MCM-41 Implementing Batch Adsorption Process: Equilibrium, Kinetics, and Thermodynamic Studies

Ammar T. Kadhum, Talib M. Albayati *
Chemical Engineering Dept., University of Technology-Iraq, Alsina'a street,10066 Baghdad, Iraq.
*Corresponding author Email: Talib.M.Naieff@uotechnology.edu.iq.

HIGHLIGHTS

- Nanoporous silica MCM-41 was very successful in removing sulfur.
- All of the MCM-41 Characteristic properties were highly improved.
- At 180 min, 70 C° and 0.4 gm of MCM-41demonstrated efficiency in removing sulfur at 29.72%.

ARTICLE INFO

Handling editor: Mustafa H. Al-Furaiji

Keywords:

Desulfurization, Adsorption; Diesel fuel Mesoporous Silica; MCM-41; Mechanism of adsorption.

ABSTRACT

In the current work, sulfur was removed from actual diesel fuel containing 1.2 wt.% sulfur from the Al-Dura Oil Refinery (Iraq), which was studied using adsorption desulfurization with the spherical mesoporous silica MCM-41. This study investigated the effects of different operating conditions, including the dose of MCM-41 (0.04-0.2 gm), time (60-180 min), and temperature (30-70°C). The optimal working conditions were determined to be 0.4 gm MCM-41, 180 min, and 70°C. After exploring the isotherm models of Langmuir, Freundlich, and Temkin, Temkin models with a correlation coefficient (R^2 = 0.9996) were selected to best represent the stable data. The kinetics of sulfur components on MCM-41 were studied using pseudo-first-order and pseudo-second-order kinetic models and intra-particle diffusion. A pseudo-first-order adsorption kinetic model with a correlation coefficient (R^2) of 0.9867 can accurately represent the adsorption process. Gibbs free energy (ΔG^o), enthalpy (ΔH^o), and entropy (ΔS^o) were calculated as thermodynamic parameters. The adsorption of total sulfur-containing compounds onto mesoporous silica was spontaneous, endothermic, and increased the irregularity of the sulfur compounds on the surface of the adsorbent. The total sulfur content of actual diesel fuel was reduced from 1.2% to 0.84%, corresponding to a desulfurization efficiency of 29.72%. Consequently, the findings of this study might be used as a starting point for future research.

1. Introduction

The desulfurization of transportation fuels (e.g., diesel) has grown more critical because most industrialized governments have passed stronger rules to limit the sulfur content of these fuels to prevent health and environmental risks [1,2]. According to the U.S. Environmental Protection Agency (EPA), sulfur levels in diesel oil should not exceed 15 mg/L [3]. The same regulations allow no more than 15% of aromatic compounds in diesel fuel [4]. The removal of organosulfur compounds from diesel fuel is a prevalent problem in the petroleum sector, and it has been researched by [5,6]. Hydrodesulfurization (HDS) is now employed to decrease sulfur levels in liquid fuels [7]. This technique requires high pressure (3-6 MPa), high temperatures (300-400°C), and a large amount of hydrogen [8]. Furthermore, this method cannot reduce thiophene sulfur compounds, such as dibenzothiophene (DBT), benzothiophene (BT), alkylated DBTs, and 4,6-dimethyl dibenzothiophene (DMDBT). All of which are found in fuels [9,10]. Desulfurization using solvent extraction [11], adsorption [12,13], photo-oxidation [14], and ionic liquid desulfurization was developed as an alternative to hydrodesulfurization to decrease the sulfur content of petroleum products [15]. Adsorption desulfurization is considered one of the most promising methods for many reasons, such as requiring mild operating conditions, producing a good desulfurization effect, and providing high selectivity to thiophene compounds [16-18]. This technique has been used to achieve ultra-clean fuels [19]. Adsorption is a mass transfer process in which free-radical molecules get bound to a surface via intermolecular forces.

It is frequently used to remove trace impurities, such as eliminating trace amounts of aromatics from aliphatic compounds [20]. The active separation procedures involve low sorbate concentrations, which can potentially remove the sulfur compounds in transportation fuels [21]. The many solids used as adsorbents to remove impurities from liquids can be classified into two

http://doi.org/10.30684/etj.2022.132385.1110
Received 14 December 2021; Accepted 07 February 2022; Available online 24 June 2022
2412-0758/University of Technology-Iraq, Baghdad, Iraq

forms: natural and industrial. Natural adsorbents include zeolites, charcoal, clays, and clay minerals. Industrial adsorbents include activated carbon, silica gel, alumina, and molecular sieves [22,23]. Mesoporous silica has attracted significant attention because of its large surface area, structural stability, and many ordered pores [24]. Mesoporous silica compounds are helpful for adsorption, catalysis, and waste treatment. The compound is a superb host for the adsorption of a wide range of shapes, sizes, and distinctive guest molecules, such as sulfur [25]. Researchers have discovered that transition metal-functionalized adsorbents might capture aromatic sulfur compounds resistant to the HDS processes via complexation [26]. Al-Zubaidi et al. [27] studied the sulfur component's adsorption from diesel fuel on granular activated charcoal (GAC). Their results showed that the sulfur content decreased by 20.9% compared to the original sample. The kinetic study demonstrated that the Langmuir isotherm was the closest fit. Ibrahim [38] investigated the desulfurization of commercial diesel fuel using activated carbon. He found that the residual sulfur level of diesel fuel was reduced from 580 to 247 ppm, resulting in a desulfurization efficiency of 57%. The kinetic analysis revealed that the pseudo-first-order model was the optimal fit, and the Freundlich isotherm exhibited the best fit. In the current study, the mesoporous silica MCM-41 was utilized as an effective adsorbent in a batch reactor (autoclave) to remove the organosulfur compounds of real diesel fuel containing a total sulfur concentration of 1.2 wt.% from the Al-Dura Oil Refinery (Baghdad, Iraq). This paper also investigated the effects of operating factors (e.g., a dose of MCM-41, time, and temperature) on the dynamics of the batch reactor. Also, this study sought insights into the mechanism of adsorption, including characterization, thermodynamic parameters, and batch adsorption with kinetic and isotherm model fitting. The findings of this study might serve as a springboard for ongoing investigations into the removal of sulfur.

2. Experimental Work

2.1 Chemicals

Real diesel fuel was obtained for testing from AL-Dura Refinery Oil. The chemicals that were used included Bromide of cetyltrimethylammonium (CTAB, 99% purity) from Sigma-Aldrich Germany, tetraethylorthosilicate (TEOS,98% purity) from Sigma-Aldrich Germany, sodium hydroxide (NaOH) from BDH England, deionized distilled water (H_2O), without additional purification. All of the compounds were utilized.

2.2 Preparation of Mesoporous MCM-41

The nanoporous MCM-41 molecular sieves were prepared by using the sol-gel process. The most common silica source for the synthesis of MCM-41 is tetraethyl orthosilicate (TEOS), and CTAB is a structural directing agent, as described in the literature [29,30]. First, make a mixture containing NaOH with a weight of 0.35 g and 30 mL of distillate water, and dissolve 1.01 g of CTAB in solution. Then, 5.78 g of TOES was added to the mixture drop by drop, under 1h of stirring at room temperature. The homogenous mixture output in the 96-hour autoclave apparatus crystallized at a constant hydrothermal temperature of 110°C. Filtration utilizing distill water removed the micro-surface agent from the solid product. The solid material produced at 40°C was dried overnight before removing the surface agent. MCM-41 was obtained after 6 hours of calcination at 550 °C, as shown in Figure1 [31].

2.3 Characterization of Mesoporous MCM-41

The structural character and crystal structure of the generated MCM-41 were studied with X-ray diffraction (XRD) (Shimadzu-6000, Japan). The scanning electron microscopy (SEM) images acquired using Zeiss equipment (Germany) analyzed the sorbents' morphology. The Fourier-transform infrared (FT-IR) spectra of the solid materials were diluted in 1 wt.% in a transmission spectrum of 4000 - 400 cm^{-1} at 4 cm^{-1} resolution regions. A desorption analyzer [Type: ASAP2020 600, Origin: USA] measured nitrogen adsorption-desorption at 77°K.

2.4 Desulfurization procedures

Batch adsorption studies were performed by mixing the appropriate amounts of MCM-41 to 50 mL of real diesel fuel with a sulfur concentration of 12000 ppm. Then, the mixture was settled in an electronic shaker (Model: BS-21, Heidolph). Origin: Germany) with a speed of 500 rpm and a temperature range of 30°C-70°C, with a 60-180 min contact time. After each run, the waste MCM-41 was centrifuged and filtered, and the filtrate was collected to determine the residual sulfur content. The content of sulfur was measured by energy-dispersive X-ray spectroscopy (Horiba Ltd., Japan) by ASTM D-4294. The percentage of removal of sulfur components was obtained using the equation [32]:

$$\%\text{Removal} = \frac{C_0 - C_e}{C_0} \times 100 \quad (1)$$

Where C_0 represents the starting sulfur content (mg L^{-1}), and Ce represents real diesel fuel's highest sulfur concentration (mg L^{-1}).

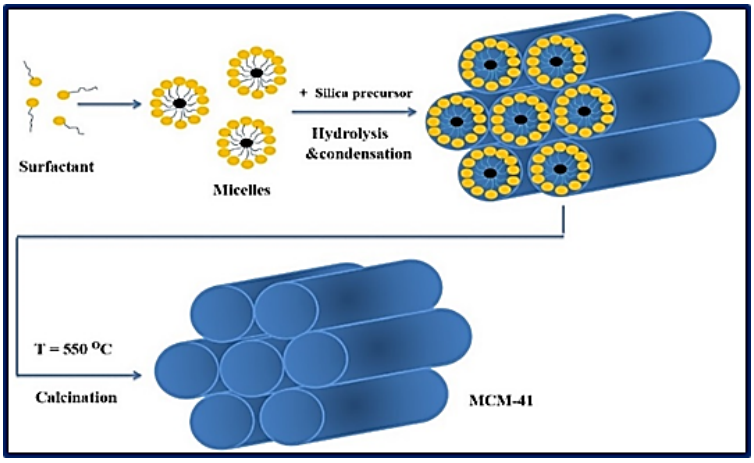

Figure 1: Scheme of synthesis of the MCM-41

3. Results and Discussions

3.1 X-RAY Diffraction (XRD)

The XRD pattern of the MCM-41synthesized Sample is shown in Figure 2. For crystalline materials, the lattice planes are usually ordered by a couple of A°, resulting in a scattering angle of 0° to 10° with a scan rate of 2 (deg/min) and Cu-k = 1.541 for atomic structure investigation. Even though amorphous materials such as mesoporous silica lack periodic atomic planes, the technique may be employed to define the ordered pore structure. The small-angle XRD pattern shows the characteristic diffraction peaks for MCM-41 of 4° and 4.4°, corresponding to planes (110) and (200). A strong diffraction peak for 100 planes at 2.4 indicates the mesoporous and existence of the channel's periodic hexagonal long-range order [33]. The position of the first peak, (1 0 0), allows a direct determination of the center-center distance between adjacent tubes using a_0 = (2*d100/√3) [34]. The calculated d_{100} and a_o values are given in Table 1. The obtained results agree fairly well with Sayari et al. [35] and Zakaria et al. [36].

3.2 Scanning Electron Microscopy (SEM)

The SEM apparatus examined the MCM-41, as shown in Figure 3a. The well-ordered hexagonal array structure of MCM-41 is seen in the SEM picture. A closer inspection of the MCM-41's surface revealed mesoporous uniform-size channels with puffy or inflated structures in a spherical shape [37]. The final result corresponded to the report's conclusions. In addition, for a sample with a mean particle size of 382.5 nm, Figure 3b displays the particle size histograms, demonstrating that the particles range in size from 50 to 50000 nm. The particle size revealed by the particle size analyzer research matched the particle size disclosed by the SEM picture.

3.3 FT.IR Spectra

To analyze the chemical compositions of MCM-41 (FT-IR, infrared Spectra) was used, as shown in Figure 4. The asymmetric stretching of Si-O-Si groups is responsible for the peaks of about 1378-1034 cm^{-1}. Furthermore, broad and weak bands at 824 and 693cm^{-1} correlate with the symmetric stretching vibration of Si-OH moieties in the pore channels. Si-OH has a broad peak between 3000 and 3900 cm1; O-H bending peaks are found at 3551 and 3402 cm^{-1}. The absorption band at 1599 cm^{-1} and 1629 cm^{-1} was ascribed to the alkyl group's C-H stretching vibration, which was observed in the spectrum of MCM-41[38]. The bands were also observed in Broyer et al. [39] and Grecco et al. [40].

3.4 BET Surface Area and Nitrogen adsorption-desorption Isotherms

The N_2 adsorption/desorption isotherm and pore size distribution investigations for MCM-41 are depicted in Figures 5 (a and b). The pore size distribution was calculated using Barrett, Joyner, and Halenda (BJH). Table 1 shows the BET surface area, average diameter, pore volume, and micropore volume of MCM-41. MCM-41 showed a substantial increase in nitrogen adsorption at P/P^o= 0.2-0.3, indicating capillary condensation of nitrogen inside the primary mesoporous structure and a narrow pore-size distribution and uniform structure. According to IUPAC categorization, the sample showed typical type IV isotherms, with hysteresis loops suggesting the representative of mesoporous materials, as shown in Figure 5a [41,42]. Figure 5b shows the pore size distribution curves, which show a single peak for the Sample. The maxima for MCM-41 were located at 2.35 nm (diameter).

Table 1: Structure properties of MCM-41

Sample	d_{100} (nm)	a_0 (nm)	S_{BET} (m^2/g)	V_p (cm^3/g)	D_{BJH} (nm)	μ_p (cm^3/g)
MCM-41	3.35	3.868	1307	0.867	2.35	0.63

Where, d_{100}: d (100) spacing, a_0: center-center distance a_0 = (2* d /√3), S_{BET}: BET surface area, V_P: pore volume, D_{BJH}: pore diameter, and μ_p: micropore volume.

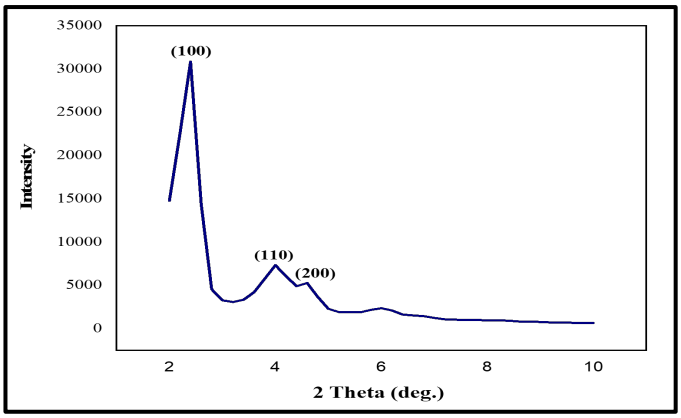

Figure 2: The produced MCM-41 adsorbent's XRD pattern

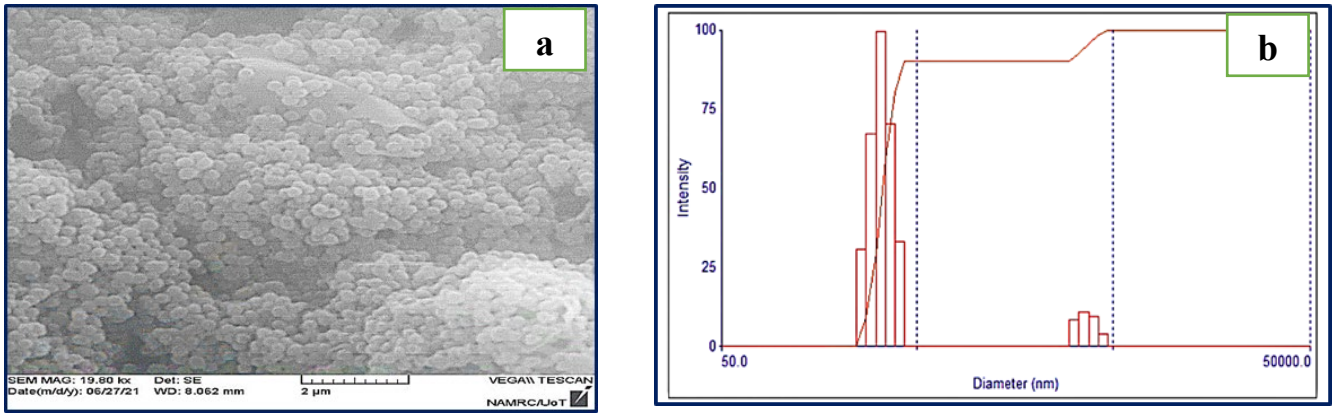

Figure 3: (a) SEM picture of MCM-41, (b) particle size distribution histogram cm^{-1}

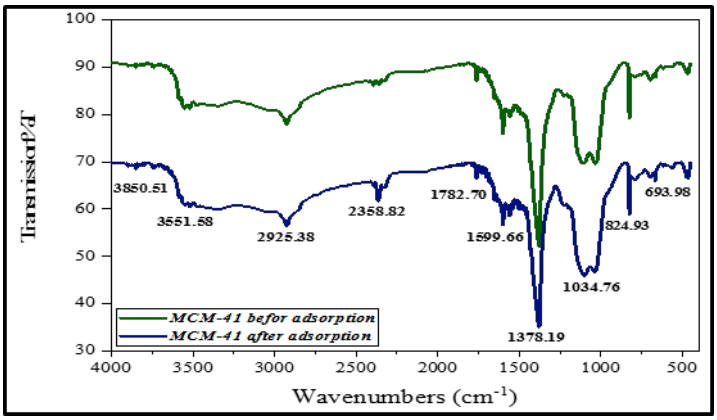

Figure 4: FT-IR spectra of MCM-41 before and after sulfur adsorption

3.5 Effect of variables

3.5.1 Effect of dose

The removal of the sulfur content increased gradually in a linear relationship to the increment of change in the sorbent dose from 0.04 to 0.2 gm, while the removal efficiency increased from 11.2 to 23.22%, as shown in Figure 6. In comparison, the removal was almost constant when raising the sorbent dose from 0.4 to 0.6 gm. The change in the adsorption of sulfur components with the rising adsorbent dose may be ascribed to the rising obtainability and availability of the surface area and the sites of adsorption to the sulfur from the diesel fuel [43]. The greater adsorption rate at the start might be due to more accessible empty spots on the adsorbent's surface. Over time, the concentration of the DBT decreased because molecules clustered into active areas, thereby reducing the accessible surface area of the MCM-41. As a result, the adsorption rate slowed. Sulfur compounds are thought to be converted to $SO4^{-2}$ and removed in the aqueous phase [44]. The findings suggest that increasing the duration of MCM-41 use can increase the adsorption capability, confirmed in the works of Rosas et al. [45].

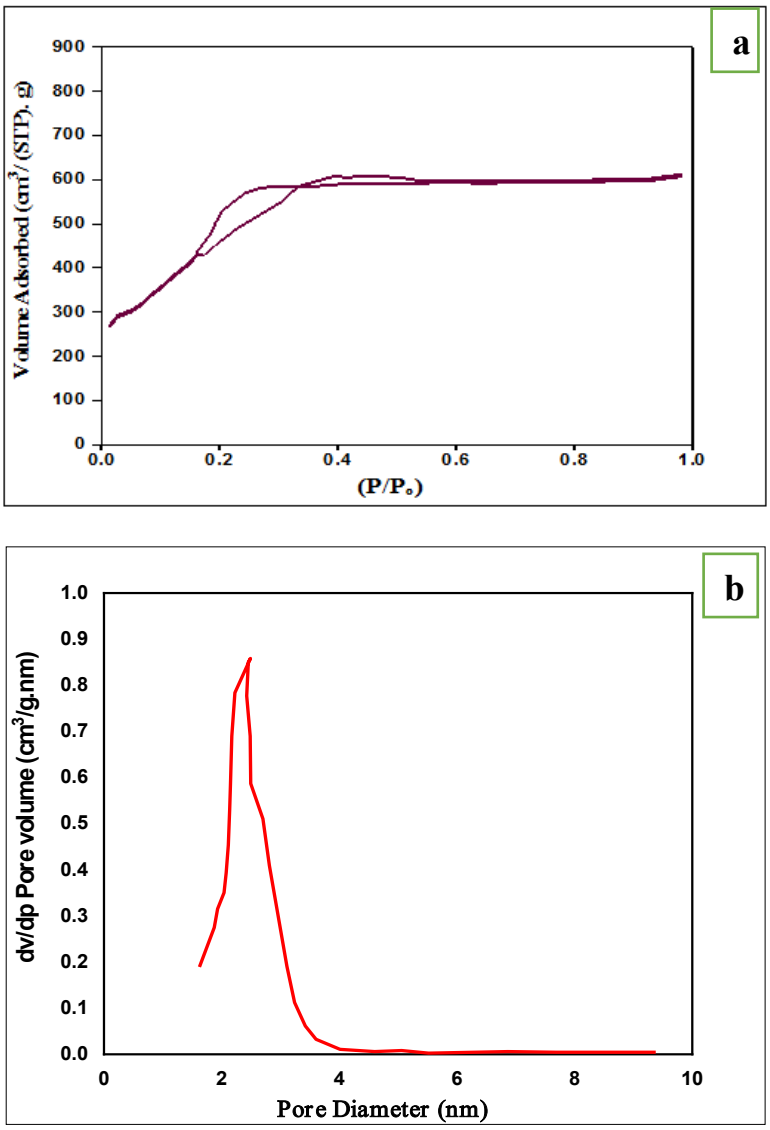

Figure 5: (a) The N2 adsorption/desorption isotherm and (b) (BJH) pore sizes distribution

3.5.2 Effect of reaction time

Preliminary experiments were conducted to determine the effect of the contact time on the sulfur concentration. This study used 50 ml of diesel fuel of 1.2 wt.% sulfur content mixed with 2. gm MCM-41 (382.5 mm particle size) at 500 rpm at 40°C. The increase in the reaction time enabled more reduction of the sulfur components, so the removal efficiency reached 25.53% after 180 min, as shown in Figure 7. Also, the amount of time spent in blending increased the contact between the phases (sulfur compounds in diesel fuel and adsorbents) when using a speed of 500 rpm. The results indicated that the residual sulfur compounds in the real diesel fuel decreased sharply during the first 60 min of treatment. With an increase in the contact time from 60 to 150 min, the residual sulfur concentration decreased gradually. However, when the contact time was increased beyond 150 min, the decrease in the residual sulfur concentration became insignificant. Equilibrium was almost attained at times greater than 150 min, which was long enough to obtain adequate sulfur removal [46]. At the start of the experiment, the adsorption rate was relatively high, which may be attributed to the availability of active sites for sulfur adsorption [47]. Because the adsorption rate decreases over time, the equilibrium state was reached after 150 min, followed by steady behavior until the experiment concluded. Although many devoid surface sites were initially available for sorption, filling the remaining devoid surface sites over time was difficult due to the repulsive interactions between the solute molecules in the solid and bulk phases. These results are consistent with Al-Zubaidy et al. (2013), who obtained acceptable sulfur reduction ranging from 410 to 251 ppm following a 2-h contact period [27].

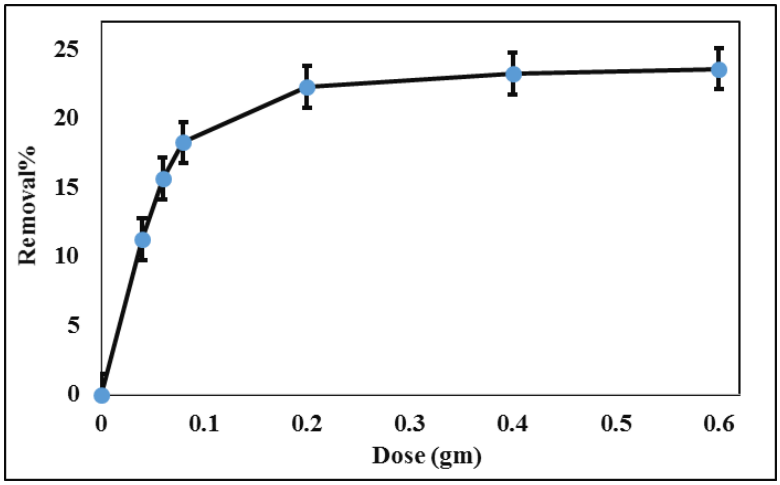

Figure 6: Sulfur content versus sorbent dose at blending speed **50**0 rpm, 40°C, and 150 min

3.5.3 Influence of reaction temperature

The effect of temperature on the desulfurization efficiency (η%) was investigated at a 180 min contact time, with 50 ml of diesel fuel, and MCM-41 particle size of 382.5 mm, a mixing speed of 500 rpm, and an initial sulfur concentration of 1.2 wt.%, as shown in Figure 8. When the adsorption temperature rose, the desulfurization efficiency also increased. The sharp decrease in desulfurization efficiency (20.4 to 26.8%) occurred by increasing the reaction temperature from 30 to 50°C. However, by increasing the adsorption temperature from 50 to 70°C, only a slight improvement in the desulfurization efficiency (26.8 to 29.7%) was obtained. It is a well-known fact that after hydrodesulfurization and having less than 1.2 wt.% sulfur, diesel fuel contains mainly refractory sulfur compounds. The increase in the number of sulfur compounds (mostly DBT) adsorbed as the temperature can be attributed to the adsorbate molecules' increased mobility in solution and within the porous sorbent structure, which allowed them to overcome the activation energy barrier [48, 49]. Music et al. (2009) discovered a similar temperature relationship based on the residual sulfur content. The batch adsorptive desulfurization of diesel oil on activated carbon was explored and improved [50].

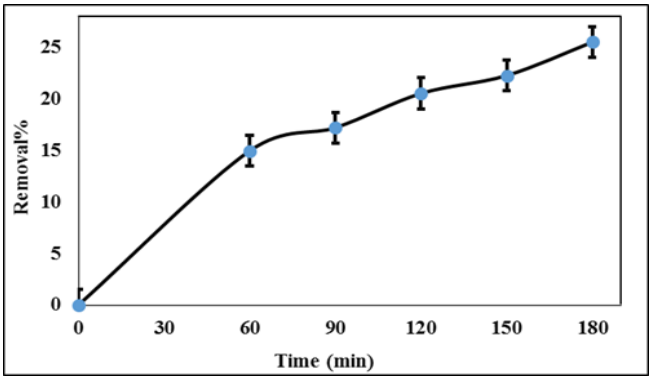

Figure 7: Sulfur content versus time at 500 rpm mixing speed, 40°C, and 0.2 gm sorbent dose

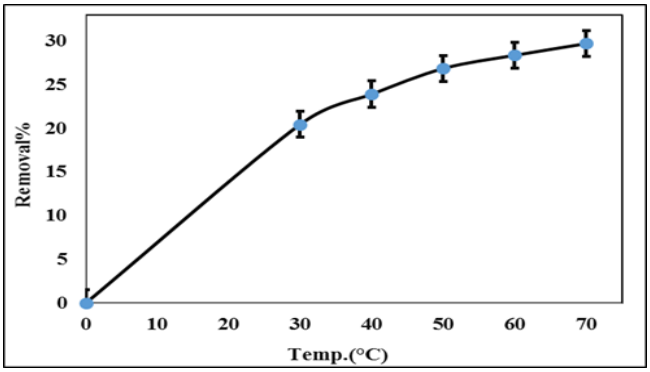

Figure 8: Sulfur content versus Temperature at 500 rpm mixing speed, 180 min and 0.4gm sorbent dose

3.6 Adsorption Isotherm Model

3.6.1 Langmuir isotherm

The Langmuir isotherm model is the monolayer adsorption on the surface of the adsorbent with a restricted no. of the adsorption sites. The model assumes that there's no adsorbate transmigration in the surface plane and that there are homogenous adsorption energies upon the surface. There is no lateral interaction among the adsorbed molecules [51]. The nonlinear Langmuir model is given in eq. (2).

$$\frac{C_e}{q_e} = \frac{1}{q_{max}} C_e + \frac{1}{q_{max}\ b} \qquad (2)$$

Where, q_{max}: Langmuir constant relates to adsorption capacity (mg/g), b: constant refers to adsorption energy (L/mg), and Ce is the concentration of adsorbate at the equilibrium (mg/L). The above constants (q_{max} and b) can be calculated from eq. (2) by plotting C_e/q_e versus C_e. are given in Table 2 and Figure 9a. Furthermore, the dimensionless equilibrium parameter R_L

presents the isotherm as favorable (R_L<1), unfavorable (R_L>1), irreversible (R_L=0), or linear (R_L=1). It is represented by eq. (3).

$$R_L = \frac{1}{1+bC_0} \quad (3)$$

C_0 in (mg/L) is the initial concentration of the sulfur.

3.6.2 Freundlich isotherm

It describes the heterogeneous (not homogeneous) process or multilayer adsorption [52], with a non-homogeneous distribution for the heat and the adsorption affinity. More robust binding sites are assumed to be initially occupied, and adsorption energy reduces with the increase in site occupancy [53]. The linear form is expressed by eq. (4):

$$\ln q_e = \ln K_f + \frac{1}{n} \ln Ce \quad (4)$$

Where, q_e is the number of analyses upon the surface of absorbent (mg/g), K_f is the constant related to the adsorption capacity of the sorbent (mg/g), and 1/n is the value that gives the favorability indication of the process of adsorption. It's a measure of adsorption intensity and surface heterogeneity that refers to the value of 1/n (0.1-1), representing favorable sorption. Figure 9b depicts the Freundlich isotherm plot, and the Freundlich constants are given in Table 2. 1/n and K_f can be determined from the slope and the intercept of the plot of $\ln q_e$ against $\ln Ce$. The comparatively high values of (R^2) remark the experimental data fitness with the model of Freundlich isotherms.

3.6.3 Temkin isotherm

Temkin isotherm assumes that the adsorption heat in the layer decreases linearly with the coverage of all adsorbate molecules because of the interactions of adsorbent and adsorbate. The absorption is eminent by a uniform energy distribution [54]. Such a model differs from Langmuir's, which includes a specific factor for the sorbent species and interactions [55]. This model is given in eq. (5):

$$q_e = B \ln K_t + B \ln Ce \quad (5)$$

Where, K_t is the equilibrium binding constant (L/g) corresponding to the maximum binding energy, B is the constant of Tempkin (J/kJ) and can be expressed by Eq. (6):

$$B = \frac{RT}{bt} \quad (6)$$

Where R is the universal gas constant (8.314 J/mol. K), T is the absolute temperature (K), and b_t is the heat of adsorption (kJ/mol).

The Temkin isotherm model best fitted the experimental data and the higher correlation coefficient (R^2 = 0.9996). Kt and b_t were determined from the intercept and the slope of the linear plot of qe versus ln Ce, as shown in Figure 9c. The b_t negative value indicates that the process is endothermic [56]. The value of (R_L = 0.4 < 1) indicates that the isotherm is favorable, and the R^2 value (0.9996) suggests that the model of Temkin to characterize the sulfur components adsorption on the MCM-41 adsorbent is better than Langmuir and Freundlich isotherm models. The Temkin constants are given in Table 2.

Table 2: Parameters of isotherm models for the desulfurization by MCM-41

Langmuir				Freundlich			Temkin		
q_{max} (mg/g)	R_L	b (L/mg)	R^2	K_f (mg/g)	1/n	R^2	b_t (KJ/mol)	K_t (L/mg)	R^2
40.485	0.4	$1.2*10^{-3}$	0.9556	$9.7*10^{21}$	0.21	0.9838	-0.001	$8.178*10^{-5}$	0.9996

3.7 Adsorption kinetics

3.7.1 First-order kinetic

The kinetic data were treated with the pseudo-first-order kinetic model. The linear form of the model is given in eq. (7) [53].

$$\log(q_e - q_t) = \log q_e - (\frac{K_1}{2.303} t) \quad (7)$$

Where qe: The sulfur adsorbed amount at the equilibrium (mg/g), qt: The sulfur absorbed amount at the time (mg/g), and K_1: The constant equilibrium rate of the pseudo-first model (min^{-1}). The rate constant K_1, the adsorbed amount at the equilibrium (qe), and the values of R^2 can be obtained from the slope and the intercept of the linear plot manifested in Table 3 and Fig 10a. The value of R^2 was equal to (0.9867), which is higher than the other kinetics. Therefore, this means that the process of adsorption was a pseudo-first-order model. Table 3 indicates that the MCM-41 simultaneous adsorption performance was comparable to some of the initial findings from other investigators [57].

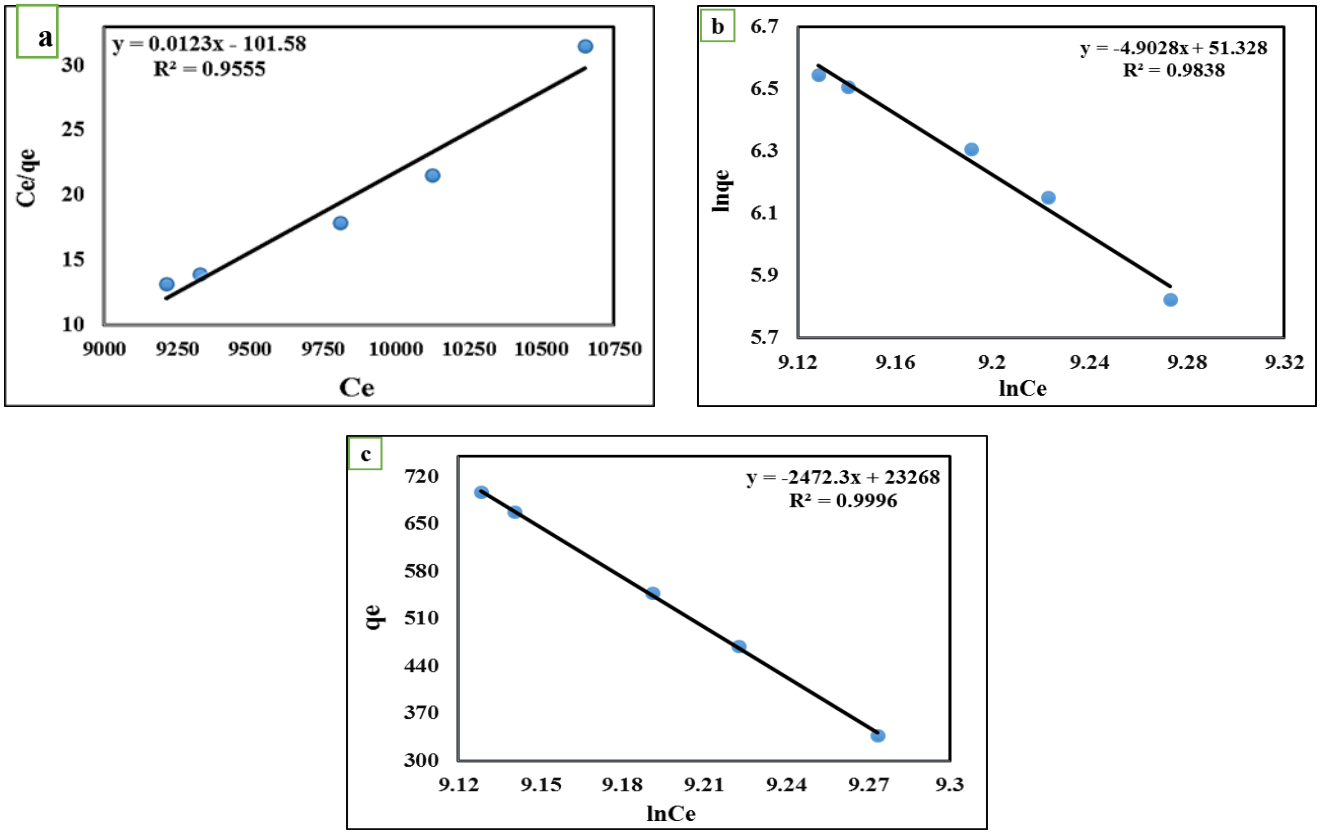

Figure 9: (a) Langmuir, (b) Freundlich and (c) Temkin isotherms

3.7.2 Second-order kinetic

The kinetic interaction of the pseudo-second-order is represented in eq. (8) [58,59].

$$\frac{t}{q_t} = \frac{1}{K_2\, q_e^{\,2}} + \frac{1}{q_e}\, t \qquad (8)$$

Where K_2 is the rate constant of pseudo-second-order for sorption (g/mg. min).

Figure 10b, (t/q_t) was plotted against the time to obtain K_2 and qe for the pseudo-second-order kinetic model. The summary of the computed values for the pseudo-second-order kinetics is given in Table 3. The values of R^2 were less than the pseudo-first-order kinetic that it was equal to (0.9649).

3.7.3 Intra-Particle diffusion

The possibility of intra-particle diffusion is represented by this model, as shown in the eq. (9) [60]:

$$q_t = K_P\, t^{0.5} + I \qquad (9)$$

Where K_P is the constant intra-particle diffusion rate of 0.5 mg/g.min, and (I) is the constant intra-particle diffusion. Figure 10c evinces that the regression lines do not pass through the origin (all points do not apply to the regression line). This indicates that the intra-particle diffusion cannot be the mere rate-determining step; thus, other processes might be involved. The values of R^2 were less than the pseudo-first-order kinetic that it was equal to (0.9844). The Intra-particle diffusion constants are given in Table 3.

Table 3: Parameters of kinetic models for the desulfurization by MCM-41

Pseudo-first order			**Pseudo-second order**			**Intra-particle diffusion**		
qe (mg/g)	K_1 (min^{-1})	R^2	qe (mg/g)	K_2 ($gmg^1\ min^{-1}$)	R^2	I	Kp ($mg/g.min^{0.5}$)	R^2
585.19	0.0035	0.9867	588.23	$1.58*10^{-5}$	0.9649	3.847	27.649	0.9844

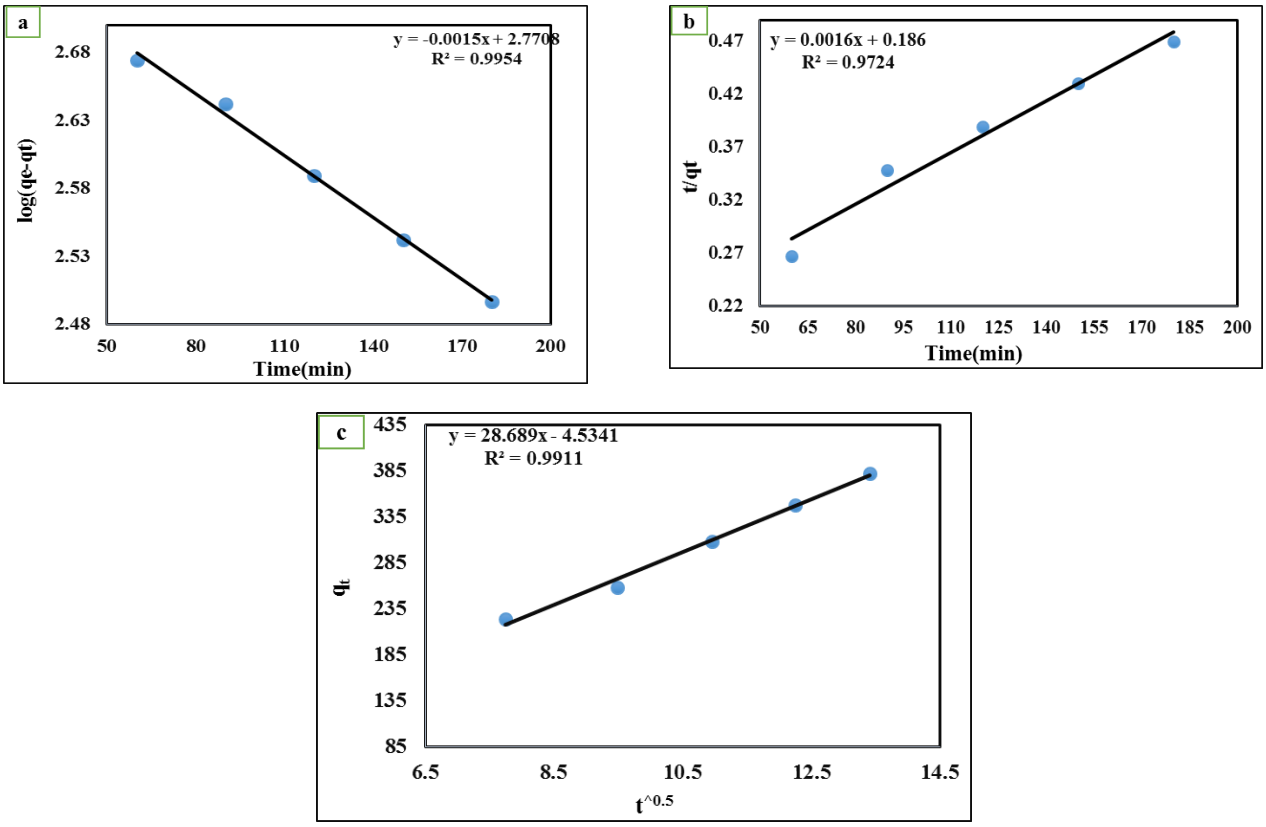

Figure 10: (a) First order, (b) Second order and (c) Intra-Particle diffusion kinetics

4. Adsorption Thermodynamics

The thermodynamics study is based on the temperature change because it is an essential factor affecting adsorption capacity. The change in the enthalpy (ΔHº), entropy (ΔSº), and Gibbs free energy (ΔGº) are the parameters of thermodynamics that can calculate the process's naturalness and viability. These parameters can be computed from the equation of Can't Hoff by using eq. (10, 11, and 12) [61]:

$$\Delta G^{o} = -RT\ln K_C \quad (10)$$

$$K_C = \frac{q_e}{C_e} \quad (11)$$

$$\ln K_C = \frac{\Delta S^{\circ}}{R} - \frac{\Delta H^{\circ}}{RT} \quad (12)$$

Where ΔSº and ΔHº (J/mol) were obtained from the slope and intercept of Van't Hoff scheme of ln K_C versus 1/T, in eq. (12). (ΔHº) and (ΔSº) were determined from the intercepts and the slopes of ln K_C versus 1/T, as revealed in Table 4 and Figure 11.

The positive values of ΔHº display that the adsorptive desulphurization process is endothermic. The positive value of ΔSº confirms the raised randomness of the sulfur molecules upon the solid surface than in the solution [62]. The sulfur components' adsorption from the treated diesel fuel was spontaneous at the investigated temperatures, as pointed out from the ΔGº negative values. The enthalpy change (ΔHº) indicates that a physisorption or chemisorption, if less than 20 KJ/mol, is physical. If it was more than 40 KJ/mol, it is chemisorption. As illustrated in Table 4, it is physisorption based on the interaction of the forces of Vander Waals.

Table 4: Thermodynamic parameters for the desulfurization by MCM-41

Temperature (Kº)	ΔHº (kJ/mol)	ΔGº (J/mol)	ΔSº (J/mol.K)
303	2.675	-4925.53	25.42
313		-5035.11	
323		-5133.12	
333		-5184.98	

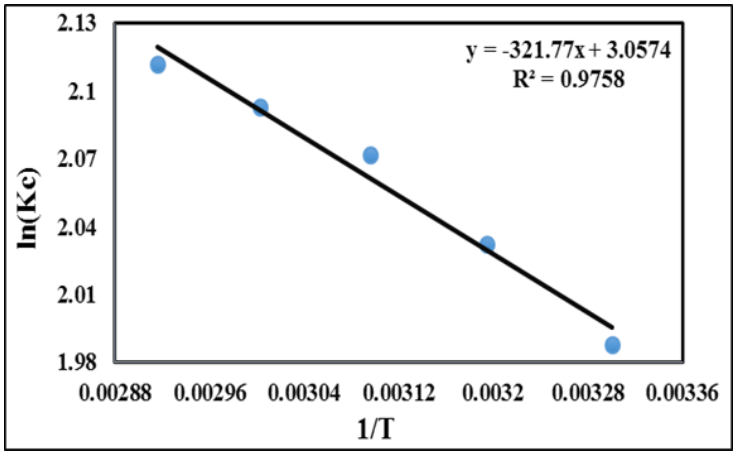

Figure 11: Thermodynamics for the desulfurization of MCM-41

5. Mechanism of Adsorption

In general, the mechanism for sulfur removal by adsorption on a sorbent material (MCM-41) is thought to entail four stages [63]: (1) movement of sulfur compounds from the bulk of the solution to the adsorbent surface (bulk diffusion); (2) movement of sulfur compounds through the boundary layer to the adsorbent surface (film diffusion); (3) movement of sulfur compounds from the particle's surface to its internal pores (intra-particle diffusion or pore diffusion); and (4) adsorption of sulfur compounds at an active spot on the material's surface (Physical adsorption via van der Waals forces). The kinetic and isotherms data were created to understand the mechanism of sulfur compounds. Given the Langmuir coefficient correlation (R^2 =0.9556), it is assumed that: (1) Adsorption is not a monolayer process (the adsorbed layer is not one molecule thick); (2) Adsorption cannot take place at a finite number of identical and equivalent definite localized places; and (3) Adsorbed molecules may form a lateral contact and produce steric hindrance even on nearby sites. Consequently, the Freundlich isotherm with 0.21< n <1 validates intra-particle diffusion and the heterogeneous surface, as does the Temkin isotherm. According to the kinetics of the Intra-particle diffusion model and the role of contact time, the adsorption of sulfur compounds by MCM-41 involves two phases, which are as follows:(1) From 0 to 90 minutes. Sulfur compounds are adsorbing on the MCM-41's exterior surface, which is the immediate adsorption stage (film diffusion); (2) From 90 to 180 minutes, sulfur compounds are contained within the MCM-41 pores (particle diffusion). Table 3 shows that, in addition to diffusion, various adsorption processes play a role in the interactions between sulfur compounds and MCM-41 particles. According to BET, SEM, and FTIR investigations, multilayer adsorption on MCM-41 is governed by surface contact (particularly with a low specific area) and by creating an intra-bond between MCM-41 and sulfur compounds, which explains the Temkin isotherm's high adsorption capacity. The adsorption mechanism is complicated in general, and it may be influenced by other parameters such as dispersive force [64], temperature [65], and ion-exchange interactions [64].

6. Batch Regeneration System

The MCM-41 sorbents' performance was evaluated with reuse testing. Following the sorption procedure, the saturated sorbent in the following run under optimal conditions. The sulfur removal percentage declined by roughly 10% in the first reuse of MCM- 41 and decreased marginally in the next three recycles, as shown in Figure 12. This might be because some surfactant templates were separated by filtering and regenerated by shaking in 0.1 M NaOH solution, centrifugation, washing, and drying at 70^{o}C. The regenerated adsorbent employed was lost from the MCM-41 surface during the initial regeneration phase, and then the loss of surfactant template decreased. As a result, the MCM-41adsorbent could be recycled several times.

7. Comparative study

This research focuses on removing sulfur compounds from actual diesel fuel using MCM-41 in a batch adsorption technique. Mesoporous silica-based materials have become important in the adsorption and treatment of real diesel fuel from sulfur compounds due to their unique properties such as medium pore size, homogeneity, and an ordered tunnel structure. Table.5 compares our work to others and shows that MCM-41 is a promising adsorbent for removing sulfur compounds in a batch system for the first time, with MCM-41 adsorption effectiveness of 29.72 percent for sulfur compounds.

Table 5: Comparison between this study and other studies

No	Sample	Adsorbent	System	sulfur Co (ppm)	% Sulfur Removal	Ref
1	Diesel fuel	Ni/MCM-41	Batch	250	58%	66
2	Diesel fuel	Ni/MCM-41	Fixed bed	450	88.8%	67
3	Diesel fuel	MCM-41	Batch	250	96.5 %	68
4	Diesel fuel	Ag/MCM-41	Batch	1234.9	95.6%	69
6	Real diesel	MCM-41	Batch	12000	29.72%	This study

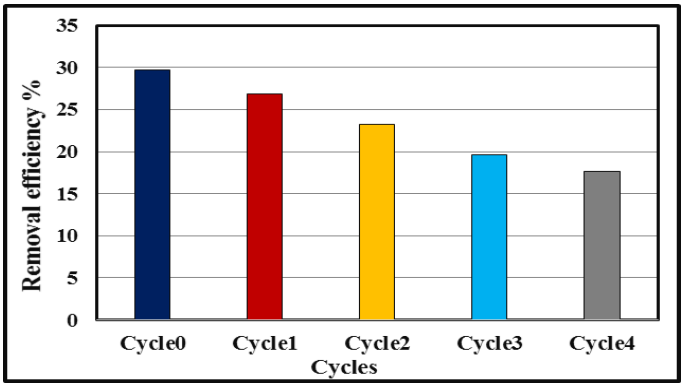

Figure 12: The reusability of MCM-41 in the batch experiment

8. Conclusion

Pure silica MCM-41 samples were successfully synthesized from silica gel, demonstrating that MCM-41 is a viable alternative adsorbent for removing sulfur-containing compounds from petroleum distillates such as real diesel fuel. Based on the present experimental study and the results obtained from adsorption desulfurization, the desulfurization efficiency improved when the time, temperature, and adsorbent dose were increased. The adsorption isotherms for the treated oil have confirmed that the desulfurization had the best fit with the Temkin isotherm model and the highest correlation coefficient (0.9996). The kinetic study also demonstrated that the optimal fit for a straight line of experimental data was achieved for the pseudo-first-order model for the adsorption desulfurization with the highest correlation coefficient (0.9867). Thermodynamic parameters, including ΔG^o, ΔH^o, and ΔS^o, were obtained in this study. They showed that the sulfur components' adsorption on the MCM-41 was spontaneous and endothermic and increased the randomness of the sulfur compounds on the adsorbent surface. The sulfur content was reduced to 0.84 wt.% under the best-operating conditions of 180 min, 70°C, 500 rpm, and 0.4 gm of MCM-41. The results revealed that MCM-41 adsorbents composed of pure silica have a high adsorption ability, where sulfur removal efficiency reached 29.72% for desulfurizing real diesel fuel.

Acknowledgment

The authors extend their gratitude to the Chemical Engineering Department at the University of Technology, Baghdad, Iraq and AL-Dura Refinery for their assistance with this study.

Author Contribution

Methodology Ammar Thamer Kadhum; Writing-Original Draft Preparation, Ammar Thamer Kadhum; Writing-Review & Editing, Talib M. Albayati. "All authors have read and agreed to the published version of the manuscript".

Funding

This research received no external funding.

Data Availability Statement

Not applicable.

Conflicts of Interest

The authors declare no conflict of interest.

References

[1] A. A. Nuhu, Bio-catalytic Desulfurization of Fossil Fuels: A Mini-Review, Rev Env. Sci, Biol., 12 (2012) 9-23. http://dx.doi.org/10.1007/s11157-012-9267-x

[2] M. Soleimani, A. Bassi, A. Margaritis, Biodesulfurization of Refractory Organic Sulfur Compounds in Fossil Fuels, Bio.Adv., 25 (2007) 570-596. https://doi.org/10.1016/j.biotechadv.2007.07.003

[3] J. Calzada, A. Alcon, V. E. Santos, F. Garcia-Ochoa, Mixtures of Pseudomonas Putida CECT 5279 Cells of Different Ages: Optimization as Biodesulfurization, Catal, Process. Biochem., 46 (2011) 1323-1328. https://doi.org/10.1016/j.procbio.2011.02.025

[4] H. H. Dabaghi, M. Kazemzad, Y. Ganjkhanlou, A. A. Yuzbashi, Electrochemical Preparation of New Organosilicon Compounds for Functionalizing of Mesoporous Silica, Funct. Mater. Lett., 6 (2013) 1350031-1350034. https://doi.org/10.1142/S1793604713500318

[5] H. H. Andevary, A. Akbari, M. Omidkhah, highly efficient and selective oxidative desulfurization of diesel fuel using dual-function [Omim] FeCl4 as catalyst/extractant, Fuel. Process. Technol., 185 (2019) 8–17. https://doi.org/10.1016/j.fuproc.2018.11.014

[6] R.-M. Gao, J.-S. Zhao, Different supports of modified heteropoly acid for ultra-deep oxidative desulfurization: a newly accessible shaped catalyst and the DFT cluster model study, Fuel, 237 (2019) 840–850. http://dx.doi.org/10.1016/j.fuel.2018.10.061

[7] A. Swapnil, N. Mahesh, Varma, Z. Shende, and K. L. Was war, Synthesis, characterization and application of 1-butyl-3 methylimidazolium chloride as a green material for extractive desulfurization of liquid fuel, Sci. World J., (2013).

[8] C. Sentorun-Shalaby, S. K. Saha, C. Song, Mesoporous molecular- sieve-supported nickel sorbents for adsorptive desulfurization of commercial ultra-low-sulfur diesel fuel, Appl. Catal. B: Environ., 101 (2011) 718–726. https://doi.org/10.1016/j.apcatb.2010.11.014

[9] Y. A. Abd Al-Khodor, T. M. Albayati, Adsorption Desulfurization of Actual Heavy Crude Oil Using Activated Carbon, Eng. Technol. J., 38 (2020) 1441-1453. http// doi.org/10.30684/etj.v38i10A.615

[10] G. H. Abdullah, M. Kadhom, S. Salih, H. N. Mohammed, S. A. Gheni, and S. M. R. Ahmed, Functionalized Multiwall Carbon Nanotube Electrode for Electrochemical Oxidation of Dibenzothiophene in Diesel, Petr. Coal, 63 (2021) 3.

[11] L. Lin, L. Hong, Q. Jianhua, X. Jinjuan, Progress in the technology for desulfurization of crude oil, China Pet. Process. Petrochemical Technol., 5 (2010) 355–6.

[12] M. Shakirullah, I. Ahmad, W. Ahmad, M. Ishaq, Desulphurization study of petroleum products through extraction with aqueous ionic liquids, J. Chil. Chem. Soc., 55 (2010) 179-83. http://dx.doi.org/10.4067/S0717-97072010000200007

[13] A. Mohamed, M. R. Betiha, S. Hoda, A. Ahmed, F. Mohamed, Oxidative desulfurization using graphene and its composites for fuel containing thiophene and its derivatives: An updated review, Egypt. J. Pet., 27 (2018) 715–30. https://doi.org/10.1016/j.ejpe.2017.10.006

[14] L. Mguni, Y. Yali, L. Xinying, D. Hildebrandt, G. David, Desulphurization of diesel fuels using intermediate Lewis acids loaded on activated charcoal and alumina, Chem. Eng., 206 (2019) 572–80. https://doi.org/10.1080/00986445.2018.1511983

[15] A. Kashif, U. S. Solat, Methods for desulphurization of crude oil - a review, Sci. Int., 28 (2016) 1169–73. https://doi.org/10.1016/j.asej.2020.03.010

[16] I. Ahmed, S. H. Jhung, Composites of metal-organic frameworks: preparation and application in adsorption, Mater.Tod., 17 (2014) 136-146. https://doi.org/10.1016/j.mattod.2014.03.002.

[17] J. M. Palomino, D. T. Tran, A. R. Kareh, C. A. Miller, J. M. Gardner, H. Dong, S. R. Oliver, Zirconia-silica based mesoporous desulfurization adsorbents, J. Pow. Sou., 278 (2015)141-148. https://doi.org/10.1016/j.jpowsour.2014.12.043.

[18] T. A. Saleh, Simultaneous adsorptive desulfurization of diesel fuel over bimetallic nanoparticles loaded on activated Carbon, J. Clea. Prod., 172 (2018) 2123-2132. https://doi.org/10.1016/j.jclepro.2017.11.208

[19] M. Tymchyshyn, M, Deep desulphurization of diesel fuels, Lakehead University, (2008). https://doi.org/10.1080/10916466.2016.1202972.

[20] A. Takahashi, F. H. Yang, R. T. Yang, New sorbents for desulfurization by π-complexation: thiophene/benzene adsorption, Indu. Eng. Chem. Res., 41(2002) 2487-2496. https://doi.org/10.1021/ie0109657

[21] A. D. Hammad, Z. Yusuf, N. Al-Rasheedi, In-situ electrochemical desulfurization of crude oil and its fraction, Saudi Aramco J. Technol., (2012) 1-5. http//doi.org/10.30684/etj.v38i10A.615.

[22] H. Kalavathy, B. Karthik, L. R. Miranda, Removal and recovery of Ni and Zn from aqueous solution using activated Carbon from Hevea Brasiliense's: batch and column studies. Colloids Surf. B, 78 (2010) 291-302. https://doi.org/10.1016/j.colsurfb.2010.03.014.

[23] G. Yu, S. Lu, H. Chen, Z. Zhu, Diesel fuel desulfurization with hydrogen peroxide promoted by formic acid and catalyzed by activated Carbon, Carbon, 43 (2005) 2285-2294. https://doi.org/10.1016/j.carbon.2005.04.008.

[24] T. M. Albayati, Application of nano porous material MCM-41 in a membrane adsorption reactor (MAR) as a hybrid process for removing methyl orange, Desal. Water Treat., 151 (2019) 138–144. https://doi:10.5004/dwt.2019.23878.

[25] Y. Chen, X. Shi, B. Han, H. Qin, Z. Li, Y. Lu, Y, Kong, The Complete Control for the Nanosize of Spherical MCM-41, J. Nanosci. Nanot., 12 (2012) 7239-7249. https://doi.org/10.1166/jnn.2012.6459.

[26] H. Song, Y. Chang, H. Song, Deep adsorptive desulfurization over Cu, Ce bimetal ion-exchanged Y-typed molecule sieve, Adsorption, 22 (2016) 139–150. https://doi.org/10.1007/s1045 0-015-9731-3.

[27] I. Al Zubaidi, N. N. Darwish, Y. El Sayed, Z. Shareefdeen, Z. Sara, Adsorptive desulfurization of commercial diesel oil using granular activated charcoal, Int. J. Adv. Chem. Eng. Biol. Sci., 2 (2015) 15-18. http://dx.doi.org/10.15242/IJACEBS.C0315040

[28] M. T. Reza, S. Reza, H. Sudeh, Dynamic filtration and static adsorption of lead ions in aqueous solution using composite polysulfone membranes with nano-size MCM-41 particles coated by polyaniline, Environ. Sci. Pollut. Res., 25 (2018) 20217- 20230. https://doi.org/10.1007/s11356-018-2236-3

[29] S. M. Alardhi, T. M. Albayati, J. M. Alrubaye, Adsorption of the methyl green dye pollutant from aqueous solution using mesoporous materials MCM-41 in a fixed-bed column, Heliyon, 6 (2020) e03253. https://doi.org/10.1016/j.heliyon.2020.e03253 .

[30] H. Faghihian, S. h. Naeemi, Application of a Novel Nanocomposite for Desulfurization of a Typical Organ Sulfur Compound, Iran. J. Chem. Eng., (IJCCE), 32 (2013) 9-15.

[31] T. M. Albayati and K. R. Kalash, Polycyclic aromatic hydrocarbons adsorption from wastewater using different prepared mesoporous materials MCM-41in batch and fixed-bed column, Process Saf. Environ. Prot.., 133 (2020) 124–136. https://doi.org/10.1016/j.psep.2019.11.007

[32] Y. A. Abd Al-Khodor, T. M. Albayati, Employing sodium hydroxide in desulfurization of the essential heavy crude oil: Theoretical optimization and experimental evaluation, Process Saf. Environ. Prot.., 136 (2020) 334-342. https://doi.org/10.1016/j.psep.2020.01.036.

[33] S. M. Alardhi, J. M. Alrubaye, T. M. Albayati, Adsorption of Methyl Green Dye onto MCM-41: Equilibrium, Kinetics and Thermodynamic Studies, Desal. Water Treat.,179 (2020) 323–331. https://doi.org/10.5004/dwt.2020.25000

[34] T. Zhang, W. L. Li, X. X. Chen, H. Tang, Q. Li, J. M. Xing, H. Z. Liu, Enhanced Biodesulfurization by Magnetic Immobilized Rhodococcus Erythropolis LSSE8-1-Vgb Assembled with Nano-γ-Al_2O_3, World J. Mic. Bio., 27 (2011) 299-305. https://doi.org/10.1007/s11274-010-0459-7

[35] A. Sayari, P. Liu, M. Kruk, M. Jaroniec, Characterization of Large-Pore MCM-41 Molecular Sieves Obtained via Hydrothermal Restructuring, Chem. Mater., 9 (1997) 2499-2506.https://doi.org/10.1021/cm970128o

[36] K. Zakaria, B. Bouhadjar, K. Zahira, O. Rachida, C. Noureddine, V. Didier, H. Rachida, Key factor affecting the basicity of mesoporous silicas MCM-41: effect of surfactant extraction time and Si/Al ratio, Chem. Papers., (2017) 1-12. https://doi.org/10.1007/s11696-017-0279-4

[37] T. M. Albayati, A. A. Jassam, Experimental Study of Drug Delivery system for Prednisolone Loaded and Released by Mesoporous Silica MCM-41, Al-Khwarizmi Eng. J., 15 (2019) 117- 124. https://doi.org/10.22153/kej.2019.06.004

[38] T. M. Albayati, A. M. AlKafajy, Mesoporous Silica MCM-41 as a Carriers Material for Nystatine Drug in Delivery System, Al-Khwarizmi Eng. J., 15 (2019) 34- 43. https://doi.org/10.22153/kej.2019.11.003

[39] M., Broyer, S., Valance, J. P. Bellat, O. Bertrand, G. Weber, Z. Gabelica, Influence of ageing, thermal, hydrothermal, and mechanical treatments on the porosity MCM-41 mesoporous silica, Langmuir, 18 (2002) 5083-5091. https://doi.org/10.1021/la0118255

[40] S. T. Grecco, U. Ernesto, E. Reyes, M. Opurtus, Influence of Temperature and Time of seed ageing on the properties of beta zeolite/MCM-41 material, J. Brazilian Chem. Soci., 25 (2014) 2445- 2353. https://doi.org/10.5935/0103-5053.20140271

[41] J. Ortiz-Bustos, A. Martín, V. Morales, R. Sanz and R. A. García-Muñoz, Surface-functionalization of mesoporous SBA-15 silica materials for controlled release of methylprednisolone sodium hemi succinate: Influence of functionality type and incorporation strategies, Microporous Mesoporous Mater, 240, (2017) 236-245. https://doi.org/10.1016/j.micromeso.2016.11.021

[42] P. V. Shah, and S. J. Rajput, A comparative in vitro release study of raloxifene encapsulated ordered MCM-41 and MCM-48 nanoparticles: a dissolution kinetics study in simulated and biorelevant media, J. Drug. Del. Sci. Technol., 41, (2017) 31-44. https://doi.org/10.1016/j.jddst.2017.06.015

[43] A. Adeyi, F. Abekanmi, Comparative analysis of adsorptive desulphurization of crude oil by manganese dioxide and zinc oxide, Rese. J. of Chem. Scie., 2 (2012)14-20.

[44] S. Houda, C. Lancelot, P. Blanchard, L. Poinel, C. Lamonier, Oxidative Desulfurization of Heavy Oils with High Sulfur Content: A Review, Catal., 8 (2018) 344. https://doi.org/10.3390/catal8090344

[45] C. Marín-Rosas, L. F. Ramírez-Verduzco, F. R. Murrieta-Guevara, G.Hernandez-Tapia, L. M Rodríguez-Otal, Desulfurization of low sulfur diesel by adsorption using activated carbon: adsorption isotherms, Indus. Eng. chem. Rese., 49 (2010) 4372-4376.https://doi.org/10.1021/ie901756b

[46] N. K. Ibrahim, S. K. Aljanabi, Desulfurization and kinetic study of diesel fuel by batch adsorption on activated carbon, Eng. . Technol. J., 33 (2015). http//doi.org/10.30684/etj.v38i10A.615

[47] S. H. Azman, A. Afandi, B. Hameed, A. M. Din, Removal of Malachite Green from Aqueous Phase Using Coconut Shell Activated Carbon: Adsorption, Desorption, and Reusability Studies, J. Appl. Sci. Eng., 21(2018) 317-330. https://doi.org/10.6180/jase.201809_21(3).0003

[48] S. M. Jabbar, Desulfurization of Al-Ahdab Crude Oil using Adsorption-Assisted Oxidative Process, PhD Thesis, University of Technology, (2013).

[49] S. Velu S. Velu, Ma. Xiaoliang, C. Song, Selective adsorption for removing sulfur from jet fuel over zeolite-based adsorbents, Ind. Eng. Chem. Rese., 42 (2003) 5293-5304. https://doi.org/10.1021/ie020995p

[50] M. M. Muzic, Z. Gomzi, K. Sertic-Bionda, Analysis of continuous fixed bed adsorptive desulfurization of diesel fuel, Faculty. Chem. Eng. Tech., (2009).

[51] I. Langmuir, The constitution and fundamental properties of solids and liquids, Part I. Solids, J. Am. Chem. Soci., 38 (2016) 2221-2295. https://doi.org/10.1021/ja02268a002

[52] K. Vijayaraghavan, T. V. N. Padmesh, K. Palanivelu, M. Velan, Biosorption of nickel (II) ions onto Sargassum wightii: application of two-parameter and three-parameter isotherm models, J. Hazard. Mater., 133 (2006) 304-308. https://doi.org/10.1016/j.jhazmat.2005.10.016

[53] G. I. Danmaliki, T. A. Saleh, Effects of bimetallic Ce/Fe nanoparticles on the desulfurization of thiophenes using activated Carbon, Chem. Eng. J., 307 (2017) 914-927. https://doi.org/10.1016/j.cej.2016.08.143

[54] M. A. Al-Ghouti, D. A. Dana, Guidelines for using and interpreting adsorption isotherm models: A review, J. Hazard. Mater. 122383 (2020). https://doi.org/10.1016/j.jwpe.2021.102354

[55] M. Hosseini, S. F. Mertens, M. Ghorbani, M. R. Arshadi, Asymmetrical Schiff bases as inhibitors of mild steel corrosion in sulphuric acid media, Mater. Chem. Phys., 78 (2003) 800-808. https://doi.org/10.1016/S0254-0584(02)00390-5

[56] T. A. Saleh, K. O. Sulaiman, S. A. AL-Hammadi, H. Dafalla, & G. I. Danmaliki, Adsorptive desulfurization of thiophene, benzothiophene and dibenzothiophene over activated carbon-manganese oxide nanocomposite: with column system evaluation, J. Clea. Prod., 154 (2017) 401-412. https://doi.org/10.1016/j.jclepro.2017.03.169

[57] M. Nkosi, Desulphurization of Petroleum Distillates Using Adsorption Method (Doctoral dissertation, University of the Witwatersrand, Faculty of Eng. and the Built Env., Sch. Chem. Meta. Eng., (2014).

[58] T. M. Albayati, A. A. Sabri, D. B. Abed, Functionalized SBA-15 by amine group for removing Ni (II) heavy metal ion in the batch adsorption system, Desal. Water Treat., 174 (2020) 301–310. https://doi.org/10.5004/dwt.2020.24845

[59] C. D. Smedt, F. Ferrer, K. Leus P. Spanoghe., Removal of Pesticides from Aqueous Solutions by Adsorption on Zeolites as Solid Adsorbents, Adsorpt. Sci. Technol., 33 (2015) 457-484. https://doi.org/10.1260/0263-6174.33.5.457

[60] R. G. Pratibha, P. K. Jayant, Isotherm and Kinetics of Desulphurization of Diesel by Batch Adsorption Studies, Int. J. Chem. Eng. Res., 10 (2018) 1-16. http://www.ripublication.com

[61] I. A. W. Tan, A. L. Ahmad, B. H. Hameed, Adsorption isotherms, kinetics, thermodynamics and desorption studies of 2, 4, 6-trichlorophenol on oil palm empty fruit bunch-based activated Carbon, J. Hazard. Mater., 164 (2009) 473-482. https://doi.org/10.1016/j.jhazmat.2008.08.025

[62] A. A. Olajire, J. J. Abidemi, A. Lateef, N. U. Benson, Adsorptive desulphurization of model oil by Ag nanoparticles-modified activated carbon prepared from brewer's spent grains, J. Environ. Chem. Eng., 5 (2017)147-159. https://doi.org/10.1016/j.jece.2016.11.033

[63] http://www.fpharm.uniba.sk/fileadmin/user_upload/english/Physical_Chemistry/5-Adsorption.pdf

[64] H.S. Wahab, A.A. Hussain, Photocatalytic oxidation of phenol red onto nanocrystalline TiO^2 particles, J. Nano. Chem., 6 (2016) 261-74. https://doi.org/10.1007/s40097-016-0199-9

[65] J. Zhang, C. Wu, A. Jia and B. Hu, Kinetics, equilibrium and thermodynamics of the sorption of p-nitrophenol on two variable charge soils of Southern China, Appl. Surf. Sci., 298 (2014) 95-101. https://doi.org/10.1016/j.apsusc.2014.01.130

[66] J.C. García-Martínez, H.A. González-Uribe, M.M. González-Brambila, N.F. del Río, A.López-Gaona, L.Alvarado-Perea, and J.A. Colín-Luna,. Effect of Ni on MCM-41 in the Adsorption of Nitrogen and Sulfur Compounds to Obtain Ultra-Low-Sulfur Diesel, Top. Catal., 61 (2018) 1721-1733. https://doi.org/10.1016/j.micromeso.2022.112020

[67] S. Dasgupta, P. Gupta, A. Nanoti, A.N. Goswami, M.O. Garg, E.Tangstad, Ø.B. Vistad, A.Karlsson, and M. Stöcker, Adsorptive desulfurization of diesel by regenerable nickel-based adsorbents. Fuel, 108 (2013) 184-189. https://doi.org/10.1016/j.fuel.2012.12.060

[68] O.O. Sadare, I.M. Masitha, and M.O. Daramola, April. Synthesis, Characterization and Performance Evaluation of Pure Silica MCM-41 for Effective Removal of Dibenzothiophene from Petroleum Distillate, IOP Conf. Ser.: Mater. Sci. Eng.,1107(2021) 1012041. https://doi.org/10.1088/1757-899X/1107/1/012041

[69] V Sales, H.O. Moura, A.B. Câmara, E. Rodríguez-Castellón, J.A. Silva, S.B. Pergher, L.Campos, M.M. Urbina, T.C. Bicudo, and L.S. de Carvalho, Assessment of Ag nanoparticles interaction over low-cost mesoporous silica in deep desulfurization of diesel. Catal., 9 (2019) 1-22.https://doi.org/10.3390/catal9080651